Insulated converter by high frequency transformer for solar micro systems

Pedro Filipe de Magalhães Folgado, MSc Student, Instituto Superior Técnico

***Abstract*—This work will address applications for photovoltaic systems and its purpose is to introduce a new DC-DC converter based on an existing one, forward converter, that has a better performance than the last one, despite of the lightning conditions. Thus, there will be conducted several tests subjected to different irradiance and temperature of the cell to confirm this goal.**

A mathematical model was developed to represent an existing photovoltaic panel. In order to study the influence of irradiance and temperature in the photovoltaic system, these parameters are changed into different simulations.

The goal of these photovoltaic applications is to extract the maximum power out of the panel and then inject it to the electrical grid. So, a DC-DC converter is needed. First, in order to compare performances, the traditional forward converter was studied and developed and then the DC-DC converter introduced in this work. For both of them, were developed two controllers (one linear and one nonlinear) to extract the maximum power. Initially, all tests were made in Standard Test Conditions (STC).

At the exit of both DC-DC converters, was added a DC-AC converter, also called inverter, to transfer the energy of the photovoltaic system to the electrical grid.

To complete this work, the two DC-DC converters are compared in non STC conditions. Like expected, the new converter introduced here has a better performance than the existing one, despite of the lightning conditions.

***Index Terms*—Forward converter, Irradiance, Performance, Photovoltaic panel, Temperature.**

I. Introduction

The utilization of fossil fuels allowed the mass production of electric energy [1]. However, several disadvantages are credited to that kind of production, since the thermoelectric plants release several harmful gases to the health of living beings, like carbon dioxide, CO_2, which is responsible for increasing the greenhouse effect, sulfur dioxide, SO_2, which can contribute to acid rain, and nitrogen oxides, NO_x, which can contribute to photochemical smog phenomena and also acid deposition. Particles can also be released which, together with the sulfur dioxide, may cause respiratory problems [2]. In Portugal there is one more disadvantage, since so far there hasn't been discovered a viable way to extract fossil, which leads to a huge investment to import them. This way alternatives energies were needed. These energies come from natural resources that are constantly renewed, in a sustainable way, even after being used to generate electricity or heat [3].

This work explores solar energy, since the energy delivered by the sun to earth is approximately $4.6\times10^{20} J/hour$ [4]. In order to convert the solar energy to electric energy, it's used crystalline silicon photovoltaic cells, used by 87% of the photovoltaic technology share [4]. However, to deliver energy to the grid more power is required, and for that the photovoltaic cells are electrically connected in series and/or parallel, reaching a photovoltaic module. To increase the voltage even higher, the modules are arranged in multiple arrays. An inverter is required, since the electrical quantities are DC and we need them to be AC to transfer energy to the electrical grid. So, for each photovoltaic panel, it is used a DC-DC converter followed by a DC-AC inverter as the figure below shows:

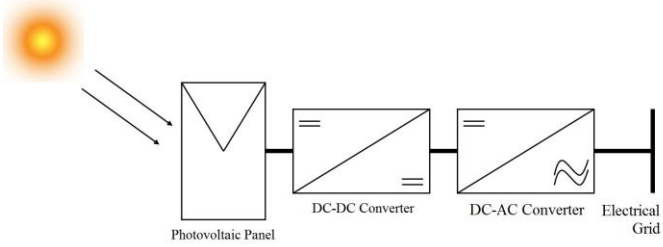

Figure 1 - Schematic of the different systems used in this work

II. Photovoltaic Panel

In order to study the behavior of the photovoltaic panel under different lightning conditions (irradiance and temperature), a mathematical model was developed in a software called Matlab, toolbox Simulink. The mathematical model chosen to incorporate this work is the "one diode and three parameters":

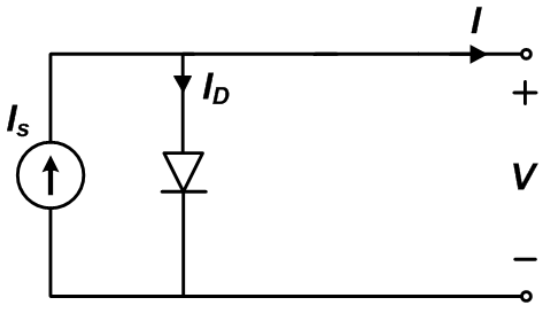

Figure 2 - Equivalent electrical circuit of a photovoltaic cell

The photovoltaic panel is the PV- MLU250HC from Mitsubishi, with 60 cells connected in series and 4 arrays cut in half. Table 1 shows some of the electrical quantities provided by the panel's manufacturer, in Standard Test Conditions ($G^r = 1000W/m^2$, $T_c^r = 25 + 273.15\ K$):

Peak Power, P_p	250 W_p
Short circuit Current, I_{sc}	8.79 A
Open circuit Voltage, V_{oc}	37.6 V
Maximum Power Voltage, V_{MP}	31 V
Maximum Power Current, I_{MP}	8.08 A

Table 1 - Electrical quantities provided by the panel's manufacturer

The three parameters (m, I_0, I_S) of this model were calculated for Standard Test Conditions as follows [3]:

$$m = \frac{V_{MP}^r - V_{ca}^r}{V_T^r \ln\left(1 - \frac{I_{MP}^r}{I_{cc}^r}\right)} \quad (1)$$

$$I_0^r = \frac{I_{cc}^r}{e^{\frac{V_{ca}^r}{mV_T^r - 1}}} \quad (2)$$

$$I_S^r = I_{cc}^r \quad (3)$$

It is assumed that the short circuit current I_{cc}, includes the irradiance variations and the reverse saturation current I_0, includes the temperature variations. On the other hand, the ideality factor m, is assumed constant along this model. To consider these changes, two new equations were obtained to I_0 and I_{cc}:

$$I_0 = I_0^r \left(\frac{T_c}{T_c^r}\right)^3 e^{\frac{N_s \varepsilon}{m}\left(\frac{1}{V_T^r} - \frac{1}{V_T}\right)} \quad (4)$$

$$I_{cc} = I_{cc}^r \frac{G}{G^r} \quad (5)$$

Table 2 shows some of the results obtained with this model in Matlab Simulink and compares them with the same electrical quantities present in the panel's manufacturer.

	Datasheet	Developed Model	Error
$V_{MP}^r\ [V]$	31.0	30.92	0.26%
$I_{MP}^r\ [A]$	8.08	8.10	0.25%
$P_p\ [W]$	250	250.49	0.20%

Table 2 – Comparison, at the maximum power point, between the values provided by the manufacturer and the values obtained by the mathematical model

The mathematical model adopted in this work to represent the photovoltaic panel is considered good, since the error is very low. Figures 3 and 4 represent the influence of irradiance and temperature on maximum power:

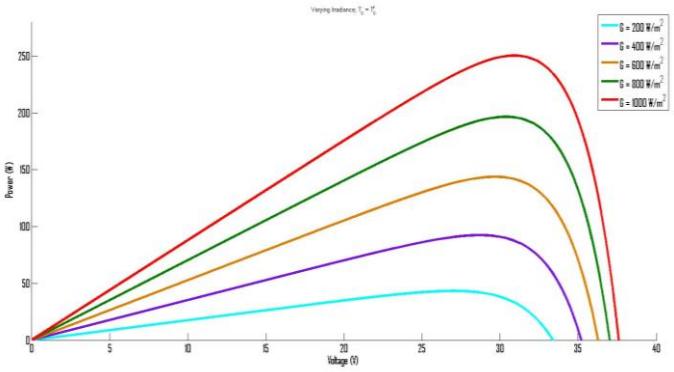

Figure 3 - Effect of irradiance on P-V curves

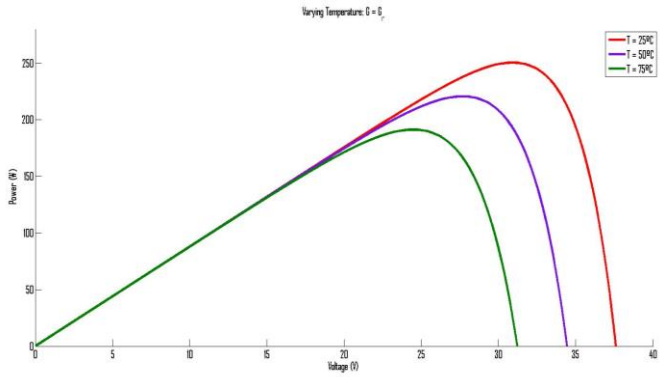

Figure 4 - Effect of temperature on P-V curves

We can easily conclude from figure 3 that the maximum power is heavily affected by changes in irradiance, because maximum power current is proportional to irradiance and maximum power voltage stays approximately constant, and from figure 4, that the maximum power is much less affected by changes in temperature.

III. FORWARD CONVERTER

The DC-DC converter responsible to increase the maximum power voltage of the photovoltaic panel is the forward converter. This converter simple topology can be obtained from the buck converter by replacing the output inductor by the primary winding of a transformer and adding to the secondary and primary windings power semiconductors to fulfill the primary and secondary circuits topological restrictions, while preventing the saturation of the magnetic core [5].

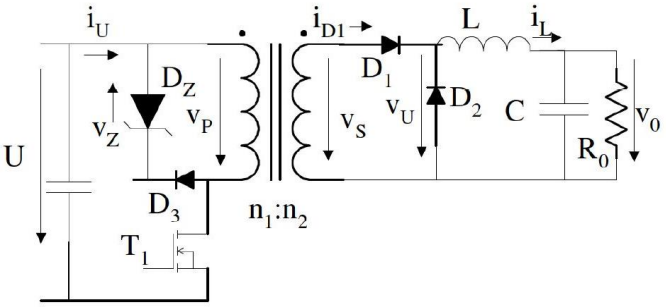

Figure 5 - Forward converter schematic

The voltages and currents of the forward converter are represented, to describe the operation principle:

$$0 < t < t_{ON} = \delta T \\ T_1\ ON,\ D_1\ ON \rightarrow \begin{cases} v_p = U \rightarrow v_{AKD3} = -U \\ i_{T1} = i_U;\ i_\mu = \dfrac{U}{l_\mu} t \rightarrow i_U = i_\mu + i_L \dfrac{n_2}{n_1} \\ v_s = \dfrac{n_2}{n_1} U \rightarrow v_U = \dfrac{n_2}{n_1} U \end{cases}$$

$$t_{ON} < t < t_{ON} + t_\mu \\ T_1\ OFF,\ D_1\ OFF \\ D_2,\ D_3,\ D_Z\ ON \rightarrow \begin{cases} v_p = -V_Z \rightarrow v_{AKD3} \approx 0 \\ i_U = 0;\ i_\mu = \dfrac{U}{l_\mu} t_{ON} - \dfrac{V_Z}{l_\mu}(t - t_{ON}) \\ v_s = -\dfrac{n_2}{n_1} V_Z \rightarrow v_U = 0; v_{AKD1} = v_s \end{cases}$$

$$t_{ON} + t_\mu < t < T \\ D_2\ ON \rightarrow \begin{cases} v_p = 0 \\ i_U = 0;\ i_\mu = 0 \rightarrow\ i_L \approx I_o \\ v_s = 0 \rightarrow v_U \approx 0 \end{cases} \quad (6)$$

In order to extract the maximum power of the photovoltaic panel, it's necessary to control the current at the output inductor and the voltage at the input capacitor. This way two controllers were designed, one linear and another non-linear. By observing the P-V curves, we realize that the maximum power voltage is obtained when the derivative is null:

$$\frac{dP}{dV} = 0 \rightarrow I_p + V_p \frac{dI_p}{dV_p} \leftrightarrow \\ \leftrightarrow V_{p\,ref}(t) \approx \\ \approx -I_p(t) \frac{V_p(t) - V_p(t - \Delta t)}{I_p(t) - I_p(t - \Delta t)} \quad (7)$$

where Δt is the time interval between samples.

After scaling all components that compose this converter, simulations were ran to check the performance of both controllers when subjected to Standard Test Conditions, STC.

Forward Converter with non-linear controller	
V_{MP} [V]	30.92
I_{MP} [A]	8.10
V_o [V]	400
I_o [A]	0.58
P_o [W]	232
η	93%

Table 3 - Electrical quantities using the non-linear controller for the forward converter

Forward Converter with linear controller	
V_{MP} [V]	31
I_{MP} [A]	8.07
V_o [V]	403.5
I_o [A]	0.57
P_o [W]	230
η	93%

Table 4 - Electrical quantities using the linear controller for the forward converter

Since the forward converter performance is very similar for both controllers, only the results of the non-linear are represented. The input current of the forward converter is the result of the sum of two currents: The secondary current transformed by the transformer and the magnetizing current.

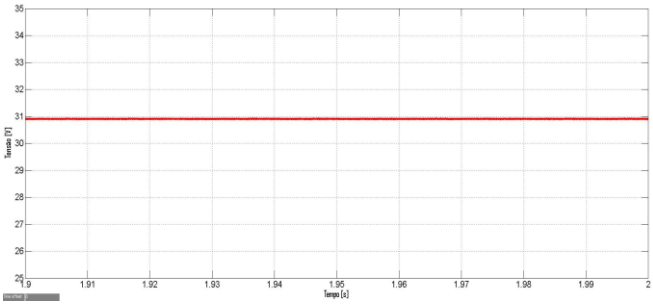

Figure 6 - Input Voltage of the forward converter (Maximum power voltage)

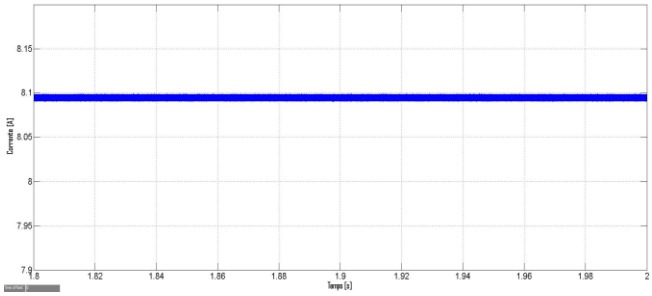

Figure 7 - Maximum Power Current of the photovoltaic panel

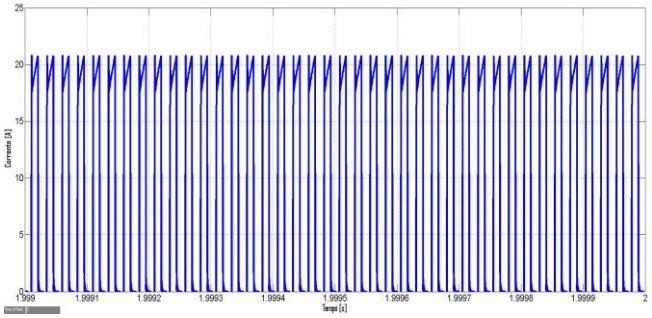

Figure 8 - Input current of the forward converter

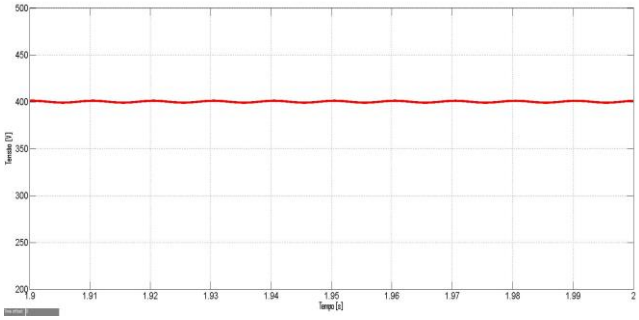

Figure 9 - Output Voltage of the forward converter

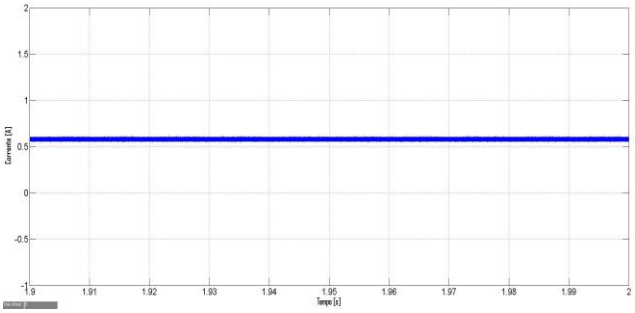

Figure 10 - Output current of the forward converter

IV. MODIFIED FORWARD CONVERTER

The objective of this new converter is to increase the efficiency of the traditional forward. With that in mind, the diode and Zener diode in the primary side were replaced by a capacitor and another MOSFET. Since the Zener diode is dissipative and the capacitor can store energy and later give it back to the system, the energy losses will decrease and the efficiency of the new converter will increase.

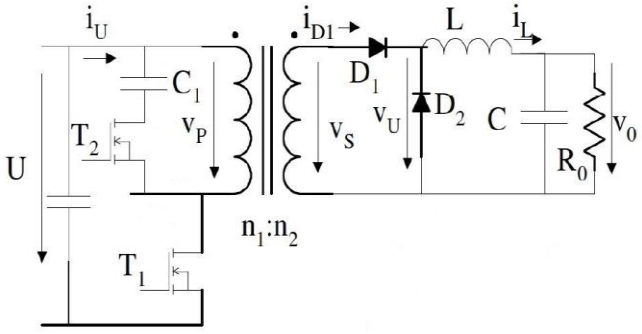

Figure 11 - Modified Forward converter schematic

The voltages and currents of the DC-DC converter are represented, to describe the operation principle:

$$0 < t < t_{ON} = \delta T \\ T_1\ ON,\ \ D_1\ ON \rightarrow \begin{cases} v_p = U \rightarrow v_{C1} + v_{T1} = -U \\ i_{T1} = i_U;\ i_\mu = \dfrac{U}{l_\mu} t \rightarrow i_U = i_\mu + i_L \dfrac{n_2}{n_1} \\ v_s = \dfrac{n_2}{n_1} U \rightarrow v_U = \dfrac{n_2}{n_1} U \end{cases} \tag{8}$$

$$t_{ON} < t < T \\ T_1\ OFF,\ \ D_1\ OFF \\ D_2,\ \ T_2\ ON \rightarrow \begin{cases} v_p = -V_{C1} \rightarrow v_{T2} \approx 0 \\ i_U = 0;\ i_\mu = \dfrac{U}{l_\mu} t_{ON} - \dfrac{V_{C1}}{l_\mu} (t - t_{ON}) \\ v_s = -\dfrac{n_2}{n_1} V_{C1};\ v_U = 0;\ v_{AKD1} = v_s \end{cases}$$

The controllers used in this new DC-DC converter are the same. After scaling the new components that integrate this converter, simulations were ran to check the performance of both controllers when subjected to Standard Test Conditions, STC.

Modified Forward Converter with non-linear controller	
V_{MP} [V]	30.93
I_{MP} [A]	8.09
V_o [V]	404.5
I_o [A]	0.59
P_o [W]	239
η	95%

Table 5 - Electrical quantities using the non-linear controller for the modified forward converter

Modified Forward Converter with linear controller	
V_{MP} [V]	31
I_{MP} [A]	8.07
V_o [V]	404.1
I_o [A]	0.59
P_o [W]	239
η	95%

Table 6 - Electrical quantities using the linear controller for the modified forward converter

Once again, since the forward converter performance is very similar for both controllers, only the results of the non-linear are represented.

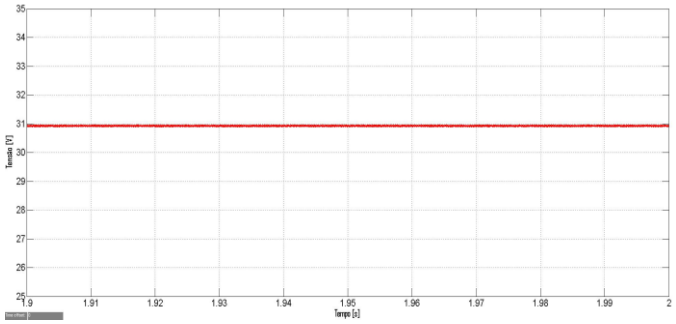

Figure 12 - Input Voltage of the new DC-DC converter (Maximum power voltage)

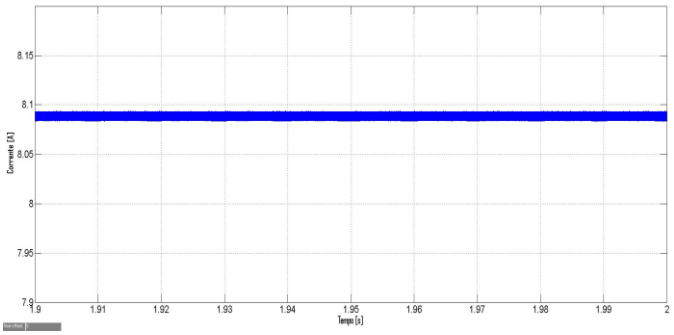

Figure 13 - Maximum power current of the photovoltaic panel

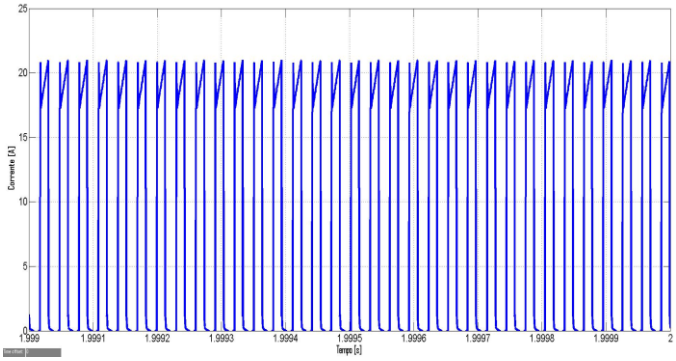

Figure 14 - Input current of the new DC-DC converter

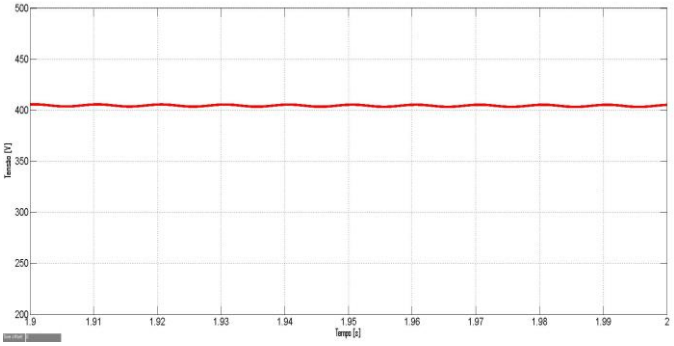

Figure 15 - Output voltage of the new DC-DC converter

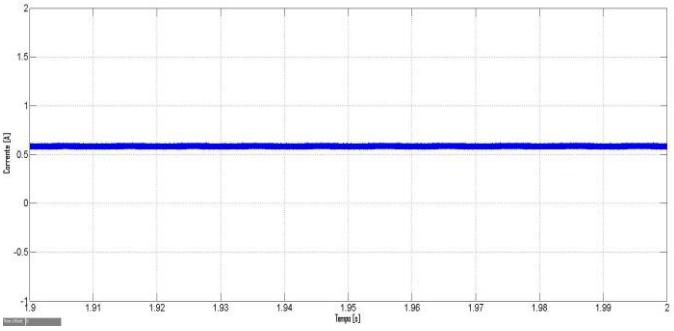

Figure 16 - Output current of the new DC-DC converter

V. INVERTER

To inject the power produced by the photovoltaic panel into the electrical grid, it is necessary to convert the DC voltage to an AC voltage. For that purpose, was used a DC-AC converter, also called inverter. In this work it was used a single-phase full-bridge inverter [6].

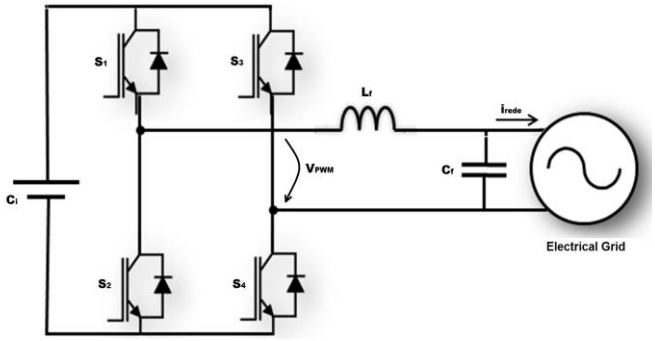

Figure 17 - Schematic of the single-phase full-bridge inverter

Since the command of the semiconductors used in this work is done through pulse width modulation of 3 levels, a function γ_{inv} to set ON and OFF the semiconductors was created [7]:

$$\gamma_{inv} = \begin{cases} 1, & if\ S_1 \wedge S_4\ ON \\ 0, & if\ S_1 \wedge S_3\ ON \vee S_2 \wedge S_4\ ON \\ -1, & if\ S_2 \wedge S_3\ ON \end{cases} \quad (9)$$

Which results for the inverter output voltage:

$$V_{PWM} = \begin{cases} V_o, & if\ S_1 \wedge S_4\ ON \\ 0, & if\ S_1 \wedge S_3\ ON \vee S_2 \wedge S_4\ ON \\ -V_o, & if\ S_2 \wedge S_3\ ON \end{cases} \leftrightarrow \quad (10)$$

$$\leftrightarrow V_{PWM} = \gamma V_o$$

To guarantee that the average value of the input voltage is practically constant and the output current has an approximately sinusoidal progress, it's necessary to build a controller for the DC-AC converter. This controller will have a linear control of the input voltage with a non-linear control of the output current.

To simulate the electrical grid, it was considered a very simple equivalent model, represented in figure 18:

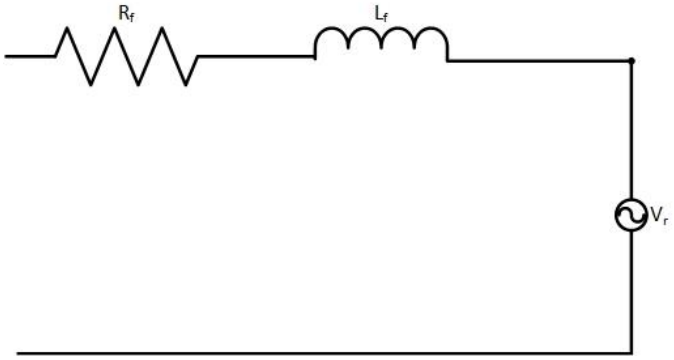

Figure 18 - Equivalent model of the electrical grid (LV)

The output inductor and capacitance is a LC filter, with the scope of reducing the harmonics with order above one. The filter's cut-off frequency ω_c was designed to be ten times the nominal grid frequency and the damping coefficient $\zeta = \frac{\sqrt{2}}{2}$:

$$L_f = \frac{2R_{eq}\zeta}{\omega_c} \quad (11)$$

$$C_f = \frac{1}{2R_{eq}\omega_c\zeta} \quad (12)$$

The electrical grid was scaled according to [8, 9] and was chosen a cable length of 500m.

After modeling the semiconductors, simulations were run to check the results:

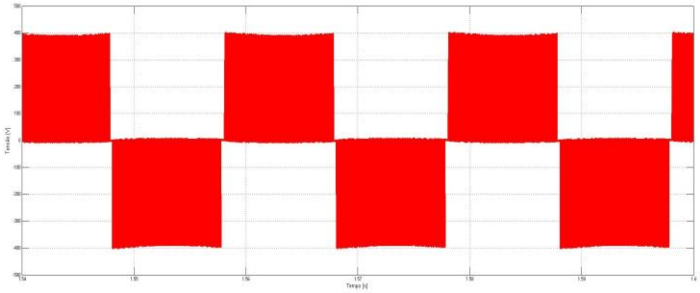

Figure 19 - Output voltage of the inverter

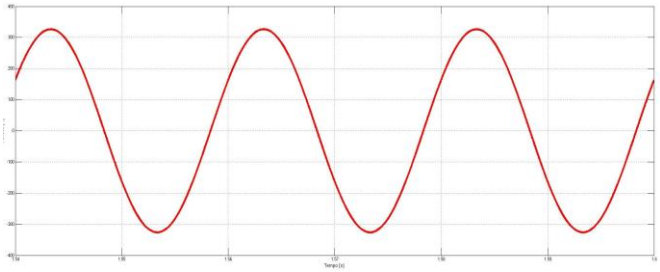

Figure 20 - Output voltage of the filter

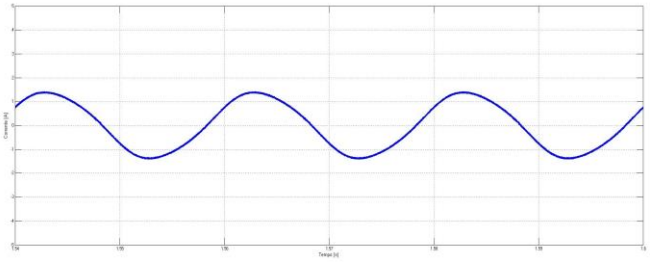

Figure 21 - Output voltage of the filter/inverter

Measuring the Total Harmonic Distortion (THD) of the current injected to the grid, 4.09% was obtained, which is a great value for applications of 250W like this one. All the results are as expected. The inverter's efficiency is 95.6%.

VI. Efficiency comparison for different conditions of irradiance and temperature

Since it was already proven that the new DC-DC forward converter is more efficient than the traditional one, under Standard Test Conditions (STC), the only thing missing to finish the scope of this work is to check if this conclusion holds under different lightning conditions. For that purpose, several simulations were done with different levels irradiance and temperature.

A. $G = G^r = 1000\,W/m^2\,;\ \theta_c = 50ºC$

Forward Converter with non-linear controller	
V_{MP} [V]	27.58
I_{MP} [A]	8.0
V_o [V]	400
I_o [A]	0.51
P_o [W]	204
η	93%

Table 7 - Electrical quantities using the non-linear controller for the forward converter

Forward Converter with linear controller	
V_{MP} [V]	27.68
I_{MP} [A]	7.96
V_o [V]	402
I_o [A]	0.51
P_o [W]	205
η	93%

Table 8 - Electrical quantities using the linear controller for the forward converter

Modified Forward Converter with non-linear controller	
V_{MP} [V]	27.61
I_{MP} [A]	7.99
V_o [V]	402.3
I_o [A]	0.52
P_o [W]	209
η	95%

Table 9 - Electrical quantities using the non-linear controller for the modified forward converter

Modified Forward Converter with linear controller	
V_{MP} [V]	27.68
I_{MP} [A]	7.96
V_o [V]	402.5
I_o [A]	0.52
P_o [W]	209
η	95%

Table 10 - Electrical quantities using the linear controller for the modified forward converter

B. $G = 800\,W/m^2\,;\ \theta_c = \theta_c^r = 25ºC$

Forward Converter with non-linear controller	
V_{MP} [V]	30.28
I_{MP} [A]	6.48
V_o [V]	400
I_o [A]	0.45
P_o [W]	180
η	92%

Table 11 - Electrical quantities using the non-linear controller for the forward converter

Forward Converter with linear controller	
V_{MP} [V]	30.37
I_{MP} [A]	6.46
V_o [V]	400.7
I_o [A]	0.45
P_o [W]	180
η	92%

Table 12 - Electrical quantities using the linear controller for the forward converter

Modified Forward Converter with non-linear controller	
V_{MP} [V]	30.32
I_{MP} [A]	6.47
V_o [V]	401
I_o [A]	0.47
P_o [W]	187
η	95%

Table 13 - Electrical quantities using the non-linear controller for the modified forward converter

Modified Forward Converter with linear controller	
V_{MP} [V]	30.37
I_{MP} [A]	6.46
V_o [V]	401
I_o [A]	0.47
P_o [W]	187
η	95%

Table 14 - Electrical quantities using the linear controller for the modified forward converter

C. $G = 600\,W/m^2\,;\ \theta_c = \theta_c^r = 25ºC$

Forward Converter with non-linear controller	
V_{MP} [V]	29.6
I_{MP} [A]	4.85
V_o [V]	400
I_o [A]	0.33
P_o [W]	130
η	91%

Table 15 - Electrical quantities using the non-linear controller for the forward converter

Forward Converter with linear controller	
V_{MP} [V]	29.67
I_{MP} [A]	4.84
V_o [V]	400
I_o [A]	0.33
P_o [W]	130
η	91%

Table 16 - Electrical quantities using the linear controller for the forward converter

Modified Forward Converter with non-linear controller	
V_{MP} [V]	29.63
I_{MP} [A]	4.84
V_o [V]	400
I_o [A]	0.34
P_o [W]	136
η	95%

Table 17 - Electrical quantities using the non-linear controller for the modified forward converter

Modified Forward Converter with linear controller	
V_{MP} [V]	29.67
I_{MP} [A]	4.84
V_o [V]	400
I_o [A]	0.34
P_o [W]	136
η	95%

Table 18 - Electrical quantities using the linear controller for the modified forward converter

VII. CONCLUSION

In all simulations executed, the new DC-DC converter has shown a better performance than the existing DC-DC forward converter. This is due to the fact that a dissipative component was changed by a capacitive one, like already explained. It was also proven, that the converter efficiency has a larger increase for lower irradiances. Thus, the DC-DC converter presented in this work fulfills the scope initially proposed.

For future studies it is suggested to try to increase a little more this DC-DC converter efficiency. For that, it's recommended to use a full-bridge in the secondary winding of the transformer. It is still proposed to try to build this converter in laboratory.

REFERENCES

[1] M King Hubbere. Energy from fossil fuels. 1949.

[2] EDP. Origens da Electricidade. http://www.edpsu.pt/pt/origemdaenergia/Pages/OrigensdaEnergia.aspx.

[3] APREN. Energias renováveis. http://www.apren.pt/pt/energias-renovaveis/o-que-sao/.

[4] Rui Castro. Uma Introdução às Energias Renováveis: Eólica, Fotovoltaica e Mini-Hídrica. IST Press. 2011.

[5] José Fernando Alves da Silva. Isolated DC-DC converters, Sistemas de Alimentação Autónomos – Textos de Apoio. Instituto Superior Técnico. 2009.

[6] João José Esteves Santana, Francis Labrique. Electrónica de Potência. Fundação Calouste Gulbenkian. 1991.

[7] José Fernando Alves da Silva. Electrónica Industrial: Semicondutores e Conversores de Potência. Fundação Calouste Gulbenkian. 2013.

[8] Filipa Isabel Félix Bernardes. Compensação de sobretensões originadas por sistemas de microgeração em redes de baixa tensão. Masther's thesis, Instituto Superior Técnico.

[9] Pedro Miguel Cabral Martins Carlos. Conversor electrónico distribuído para painéis fotovoltaicos granulares. Masther's thesis, Instituto Superior Técnico.